

Gradient-Free Adaptive Global Pruning for Pretrained Language Models

Guangji Bai¹ Yijiang Li² Chen Ling¹ Kibaek Kim² Liang Zhao^{1,*}

¹Emory University ²Argonne National Laboratory

*Corresponding Author

{guangji.bai, chen.ling, liang.zhao}@emory.edu

{yijiang.li, kimk}@anl.gov

Abstract

The transformative impact of large language models (LLMs) such as LLaMA and GPT on natural language processing is countered by their prohibitive computational demands. Pruning has emerged as a pivotal compression strategy, introducing sparsity to enhance both memory and computational efficiency. Yet traditional global pruning is impractical for LLMs because of scalability issues; and local pruning, despite its efficiency, leads to suboptimal solutions. Addressing these challenges, we propose adaptive global pruning (AdaGP), a novel framework that redefines the global pruning process into manageable, coordinated sub-problems, allowing for resource-efficient optimization with global optimality. AdaGP’s approach, which conceptualizes LLMs as a chain of modular functions and leverages auxiliary variables for problem decomposition, not only facilitates a pragmatic application on LLMs but also demonstrates significant performance improvements, particularly in high-sparsity regimes where it surpasses current state-of-the-art methods. The source code of AdaGP is available at <https://github.com/BaiTheBest/AdaGP>.

1 Introduction

Large language models (LLMs) (Touvron et al., 2023; OpenAI, 2023) have recently transformed the field of natural language processing by delivering exceptional results across a variety of intricate language benchmarks (Wei et al., 2022; Bommarito II and Katz, 2022; Bubeck et al., 2023). Nonetheless, these models, with billions of parameters, generally necessitate significant computational resources. To make LLMs more accessible, extensive efforts have been devoted to model compression of LLMs (Xu and McAuley, 2023; Ling et al., 2023; Bai et al., 2024), including pruning, quantization, knowledge distillation, and low-rank factorization. *Pruning*, by introducing *sparsity*, jointly enhances memory

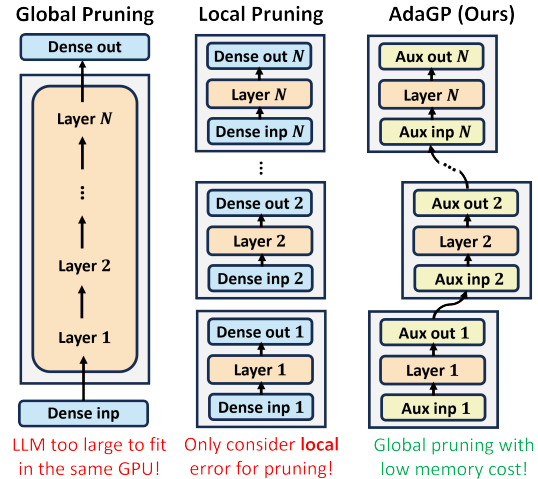


Figure 1: AdaGP decomposes the global pruning of LLMs into manageable subproblems by leveraging the chain of modules and auxiliary variables.

and computational efficiency and offers unparalleled flexibility, seamlessly integrating with any LLMs, thus standing out as a highly effective and widely adopted compression strategy.

Model pruning has a long history (LeCun et al., 1989) and has proven effective in applications related to vision and smaller language models (Hoeffler et al., 2021). However, conventional pruning techniques, which rely on global pruning and require loading the entire model into the same GPU (Mallya and Lazebnik, 2018; Singh and Alistarh, 2020), become impractical for today’s LLMs because of their vast size. Recently, several *local pruning* methods have been proposed for billion-scale LLMs. These methods compress each layer separately, and the overall compressed model is then obtained by “stitching together” the individually compressed layers. Frantar and Alistarh (2023) developed SparseGPT, an efficient unstructured pruning method for LLMs with hundreds of billions of parameters, achieving up to 60% parameter reduction with minimal performance loss. Sun et al. (2023) introduced a novel pruning criterion in Wanda, which evaluates weights by consider-

ing both magnitude and related input activations. Despite its efficiency gains, however, local pruning aims to minimize only the local error for each specific layer under sparsity constraints, and hence the final solution is *suboptimal* to the final goal of the global pruning. In other words, beyond the genuine goal of pruning, which is just to align the input and output of the pruned and original models, local pruning *overalligns* all the intermediate layers’ activations between them, resulting in a suboptimal solution, especially in high-sparsity regimes (Singh and Alistarh, 2020; Sung et al., 2023).

To address these challenges, namely, to achieve global pruning with low memory consumption, we propose adaptive global pruning (**AdaGP**), which decomposes the global pruning objective into many subproblems, each of which can be solved using few resources and can coordinate with each other toward the global pruning objective. More specifically, we first formulate LLMs as a composite function where the output of one module is the input of the next. Based on this, we reformulate the global pruning goal into its equivalent form, with auxiliary variables that facilitate its decomposition and its subproblems’ coordination. Then we propose an algorithm that achieves the alternating optimization of the subproblems of all the variables and auxiliary variables with low resource and global optimality, thanks to the closed-form solution of each subproblem. Empirically, we find that AdaGP can consistently improve the performance of local pruning methods, such as SparseGPT and Wanda, with marginal additional computational overhead. Particularly in high sparsity regimes ($> 60\%$), the perplexity can be significantly decreased by up to around 80% as compared with the state-of-the-art local pruning method SparseGPT.

This adaptability ensures that our framework can be seamlessly integrated into a wide range of LLMs and pruning methods, making it a versatile tool and useful baseline for future research exploiting the sparsity of LLMs.

2 Related Work

Pruning, a pivotal concept in machine learning that introduces sparsity into neural networks, dates back to the 1980s (LeCun et al., 1989). It gained renewed attention in the late 2010s, especially for deep neural networks, under the banner of reducing inference costs (Han et al., 2015). LLM pruning techniques can broadly be categorized into *struc-*

tured and *unstructured* prunings.

Unstructured pruning seeks to simplify the complexity of LLMs by removing certain parameters *regardless* of the model’s inherent structure. This approach typically involves setting a threshold to nullify parameters below it, leading to a model with a nonuniform sparse structure. Frantar and Alistarh (2023) developed SparseGPT, an efficient unstructured pruning method for LLMs with hundreds of billions of parameters, achieving up to 60% parameter reduction with minimal performance loss. Sun et al. (2023) introduced a novel pruning criterion in Wanda, which evaluates weights by considering both magnitude and related input activations. This approach is beneficial in linear layers of LLMs, helping identify and remove less significant weights. Tuli and Jha (2023) proposed DynaTran, a dynamic inference scheme for pruning activations at runtime, supported by a specially designed ASIC architecture, AccelTran, to enhance transformer inference throughput.

On the other hand, structured pruning involves the selective removal of groups of weights, where “group” might mean blocks of weights, filters, attention heads, or other structures conducive to hardware acceleration. Ma et al. (2023) introduced the LLM-Pruner, a framework designed for structured pruning of LLMs, which utilizes a combination of first-order data and Hessian information for effective importance estimation. This aids in identifying crucial groups for pruning. Li et al. (2023) proposed LoSparse, a novel approach combining low-rank and sparse matrix approximations to balance pruning and expressive power. Tao et al. (2023) extended this concept to pruning hidden dimensions in LLMs, including embedding layers and attention heads. Kurtic et al. (2023) presented ZipLM, a structured compression method for LLMs, optimizing for compression and accuracy while considering specific hardware constraints.

Our work falls in the category of unstructured pruning of LLMs. Our AdaGP framework avoids the *suboptimal* performance of existing methods such as SparseGPT and Wanda, which consider only an *entirely local* pruning algorithm. In Section 3 we discuss the limitations and challenges of such entirely local pruning.

3 Background

3.1 Global Pruning

Given a pretrained neural network f and inputs \mathbf{X} , global pruning aims to find a global sparsity mask \mathbf{M} and possibly updated weights $\widehat{\mathbf{W}}$ to minimize the *global loss* between the final outputs of the uncompressed and compressed model:

$$\min_{\mathbf{M}, \widehat{\mathbf{W}}} \mathcal{L}(f(\mathbf{X}; \mathbf{M} \odot \widehat{\mathbf{W}}), f(\mathbf{X}; \mathbf{W})), \quad (1)$$

where \odot denotes the *elementwise* multiplication. In addition to NP-hardness (Blumensath and Davies, 2008), however, a critical challenge in solving Eq. 1 for modern billion-scale LLMs is the huge memory requirement, which prohibits storing the entire model on a single GPU. Although some researchers (e.g., (Paszke et al., 2019; Smith et al., 2022)) have developed toolkits that enable parallelism across multiple GPUs, such a setup may require resources that are not easily accessible, raising interest in developing other pruning methods that are functional regardless of the availability of computational resources.

3.2 Local Pruning

Local pruning circumvents the memory issue mentioned above by dividing the full model compression into subproblems for each layer, ℓ , and constructing a *local loss* to measure the ℓ_2 -error between the outputs of the uncompressed and compressed layers. Hence, the local pruning can be formulated by

$$\min_{\mathbf{M}_\ell, \widehat{\mathbf{W}}_\ell} \|\mathbf{W}_\ell \cdot \mathbf{X}_\ell - (\mathbf{M}_\ell \odot \widehat{\mathbf{W}}_\ell) \cdot \mathbf{X}_\ell\|_2^2. \quad (2)$$

Although smaller than the global pruning, the local pruning still needs to optimize both the mask \mathbf{M}_ℓ and the remaining weights $\widehat{\mathbf{W}}_\ell$ and thus remains NP-hard. Therefore, using local pruning to exactly solve for larger layers is unrealistic, leading all existing methods to resort to approximations.

Mask Selection & Weight Reconstruction. A particularly popular approach is to separate the problem into *mask selection* and *weight reconstruction* (Hubara et al., 2021; Kwon et al., 2022). Concretely, this means first choosing a pruning mask \mathbf{M} according to some salient criterion, such as the weight magnitude (Zhu and Gupta, 2017), and then optimizing the remaining unpruned weights while keeping the mask unchanged. Importantly, once the mask is fixed, Eq. 2 turns into a *linear regression* problem that can be easily optimized.

Existing Solvers. Early work (Kingdon and Kingdon, 1997) applied iterated linear regression to small networks. Recently, the AdaPrune approach (Hubara et al., 2021) has shown good results for this problem on modern models via magnitude-based weight selection, followed by applying stochastic gradient descent steps to reconstruct the remaining weights. Follow-up works demonstrate that pruning accuracy can be further improved by removing the strict separation between mask selection and weight reconstruction. In addition, as we mentioned in Section 2, recent work (Frantar and Alistarh, 2023; Sun et al., 2023) has further advanced the scalability and pruning process.

3.3 What’s Wrong with Local Pruning?

As shown in Eq. 2, local pruning focuses on minimizing the error for each specific layer ℓ subject to sparsity constraints that are embedded in the mask \mathbf{W}_ℓ and weights $\widehat{\mathbf{W}}_\ell$. While the primary goal of the pruning process is to ensure that the input and output of the pruned model align closely with those of the original models, local pruning overly constrains the alignment of input and output of all the intermediate layers between the two models, leading to a performance degradation. This results in a solution that is suboptimal with respect to the global pruning problem.

4 Adaptive Global Pruning for LLMs

We present our proposed method AdaGP that can address the drawbacks of existing pruning methods by achieving a global pruning with low memory consumption. AdaGP decomposes the global pruning into many subproblems, each of which can be solved using few resources and can coordinate each other toward the global pruning objective.

4.1 Motivation

The development of AdaGP is motivated by the observation that LLMs can be formulated as a composite function such that the output of one module is the input of the next. This allows us to reformulate the global pruning goal into its equivalent form with auxiliary variables that enable the decomposition of the original problem into multiple subproblems, as detailed in Figure 2 and Section 4.2. Then we develop a resource-efficient algorithm that achieves global optimality via alternating optimization for each of the subproblems in which we obtain

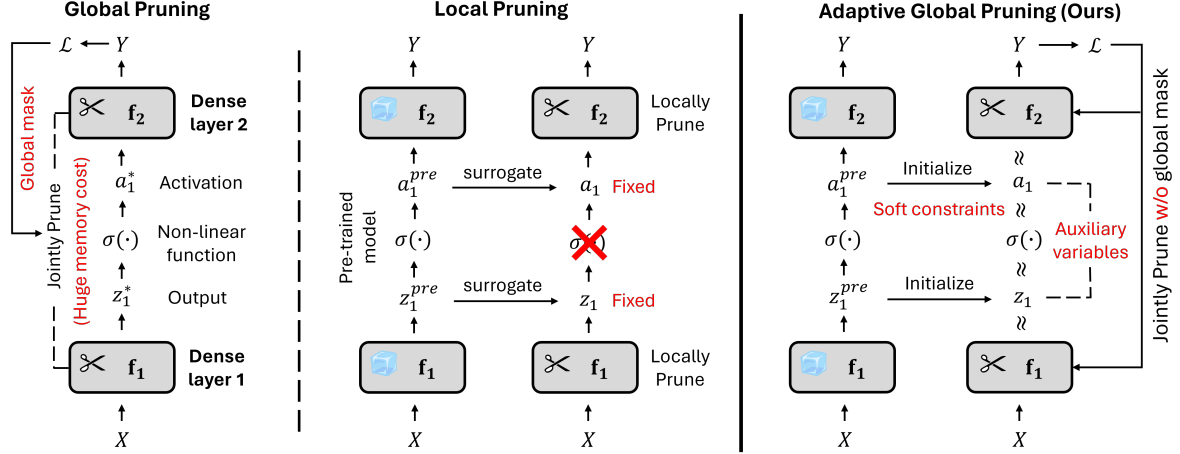


Figure 2: **Illustration of our adaptive-global pruning method** compared with *conventional global pruning* and *local pruning*. We consider a *two-layer* neural network as an abstraction for simplicity. *Global pruning* (**left**) is memory prohibitive because of poor scalability. *Local pruning* (**mid**) considers pruning each layer independently, while inevitably sacrificing performance because of the lack of global supervision. Our *adaptive global pruning* (**right**) achieves global pruning with low memory cost by leveraging auxiliary variables and soft constraints.

closed-form solutions for each of the steps. This has been illustrated in Figure 2 and Section 4.3.

4.2 A Unified Formulation of Pruning

In this section we present the reformulation of the global pruning problem into an equivalent one by introducing auxiliary variables. This reformulation enables us to swiftly shift between two extremes of global pruning and local pruning and the decomposition of the problem into many independent subproblems.

The key idea behind our reformulation is to decouple the densely parametric parts (linear layers) from the nonparametric parts (activation function, self-attention, and layer norm, etc.) using a splitting technique. Formally, given an LLM formulated as a composite function with dense layers $\ell \in [L] := \{1, 2, \dots, L\}$, where L is the total number of dense layers, we define $\Omega \subseteq [L - 1]$ to be a subset of layers for which we control the extent of globality. Note that there can be nonparametric and potentially nonlinear layers between layers ℓ and $\ell + 1$ in L , and we denote those layers by function $\phi_\ell(\cdot)$. In the reformulation, rather than feeding the output of a dense layer $\ell \in [L]$ directly into a nonparametric and potentially nonlinear layer after it, we store the output of layer ℓ in a new variable $\mathbf{z}_\ell = \mathbf{W}_\ell \mathbf{a}_{\ell-1}$,¹ where $\mathbf{a}_{\ell-1}$ is the input to layer ℓ and can be represented by $\mathbf{a}_{\ell-1} = \phi_{\ell-1}(\mathbf{z}_{\ell-1})$. Note that by definition, \mathbf{a}_0 is the input data. Con-

sequently, we can pose the pruning problem as follows:

$$\begin{aligned} & \min_{\{\widehat{\mathbf{W}}_\ell\}, \{\mathbf{M}_\ell\}, \{\mathbf{a}_\ell\}, \{\mathbf{z}_\ell\}} \mathcal{L}(\mathbf{z}_L, \mathbf{y}), \\ & \text{s.t. } \mathbf{z}_\ell = (\mathbf{M}_\ell \odot \widehat{\mathbf{W}}_\ell) \mathbf{a}_{\ell-1}, \forall \ell \in [L], \\ & \mathbf{a}_\ell = \phi_\ell(\mathbf{z}_\ell), \forall \ell \in \Omega, \\ & \mathbf{a}_\ell, \mathbf{z}_\ell = \mathbf{a}_\ell^{\text{pre}}, \mathbf{z}_\ell^{\text{pre}}, \forall \ell \in [L - 1] \setminus \Omega, \end{aligned} \quad (3)$$

where $[L - 1] \setminus \Omega$ denotes the complement set of Ω and $\mathbf{a}_\ell^{\text{pre}}$ and $\mathbf{z}_\ell^{\text{pre}}$ denote the corresponding values of \mathbf{a}_ℓ and \mathbf{z}_ℓ obtained by running a forward-propagation from the pretrained model, respectively.

In our proposed reformulation, the key to understanding its unified nature lies in the interpretation of the set Ω . The versatility of our approach is illustrated in the following remark.

Remark 4.1. *For the given LLM and definition of Ω , our formulation can seamlessly treat both global and local pruning as special cases depending on the choices of Ω . Specifically:*

- When $\Omega = [L - 1]$, solving our pruning formulation is equivalent to global pruning, accounting for interlayer dependencies across the entire network.
- When $\Omega = \emptyset$, the formulation simplifies to local pruning, considering each layer independently and ignoring interlayer dependencies.

The ability to shift between these two extremes, and potentially any intermediate configuration,

¹For the sake of simplicity and clearer presentation, the bias term is omitted in the following equations where its exclusion does not lead to confusion.

demonstrates the flexibility and comprehensiveness of our reformulation. This flexibility not only caters to a wide range of pruning strategies but also provides a unified framework to compare and contrast the effectiveness of different pruning methods under a consistent mathematical lens.

4.3 Algorithm Design

In this section we introduce a choice of Ω that achieves a good trade-off between global and local pruning, and we propose an algorithm to solve the resulting problem. Specifically, we propose an adaptive approach where global pruning is applied within each decoder layer, while still adhering to a ‘‘local pruning’’ strategy between different decoder layers. Moreover, given that the feed-forward network (FFN) module in each decoder layer accounts for more than *two-thirds* of the total parameters (Liu et al., 2024), our approach prioritizes the global pruning of these FFN layers. This strategy strikes a balance between the computational feasibility of pruning large-scale models and the effectiveness of the pruning process.

Formally, we select Ω to be the FFN layers, denoted by Ω_{FFN} . As a result, we obtain the problem of interest by substituting Ω with Ω_{FFN} in Eq. 3. We now have the following problem:

$$\begin{aligned} & \min_{\{\widehat{\mathbf{W}}_\ell\}, \{\mathbf{M}_\ell\}, \{\mathbf{a}_\ell\}, \{\mathbf{z}_\ell\}} \mathcal{L}(\mathbf{z}_L, \mathbf{y}), \\ \text{s.t. } & \mathbf{z}_\ell = (\mathbf{M}_\ell \odot \widehat{\mathbf{W}}_\ell) \mathbf{a}_{\ell-1}, \quad \forall \ell \in [L], \\ & \mathbf{a}_\ell = \phi_\ell(\mathbf{z}_\ell), \quad \forall \ell \in \Omega_{\text{FFN}}, \\ & \mathbf{a}_\ell, \mathbf{z}_\ell = \mathbf{z}_\ell^{\text{pre}}, \quad \forall \ell \in [L-1] \setminus \Omega_{\text{FFN}}. \end{aligned} \quad (4)$$

Instead of solving Eq. 4 directly, we relax the constraints by adding an ℓ_2 -penalty function to the objective to obtain an unconstrained problem. In addition, by considering the ‘‘local pruning’’ between the decoder layer, we can simplify Eq. 4 to obtain an unconstrained subproblem for each of the decoder layers as

$$\begin{aligned} & \min_{\{\widehat{\mathbf{W}}_\ell\}, \{\mathbf{M}_\ell\}, \mathbf{a}_\ell, \mathbf{z}_\ell} \alpha \|\mathbf{z}_{\ell+1}^{\text{pre}} - (\mathbf{M}_{\ell+1} \odot \widehat{\mathbf{W}}_{\ell+1}) \mathbf{a}_\ell\|_2^2 \\ & + \beta \|\mathbf{a}_\ell - \phi_\ell(\mathbf{z}_\ell)\|_2^2, \\ & + \alpha \|\mathbf{z}_\ell - (\mathbf{M}_\ell \odot \widehat{\mathbf{W}}_\ell) \mathbf{a}_{\ell-1}^{\text{pre}}\|_2^2, \end{aligned} \quad (5)$$

where α, β are hyperparameters for the penalty of the corresponding constraint in Eq. 4 and layers ℓ

and $\ell + 1$ correspond to the upscaling and downscaling linear layers in FFN. Note that for the last decoder layer, we replace $\mathbf{z}_{\ell+1}^{\text{pre}}$ with y .

In this work we consider the *alternating* method to optimize our Eq. 5, in other words, optimize each variable while keeping the rest fixed. The careful and elaborate design of our Eq. 5 allows us to derive a *closed-form* solution for each of the variables.

Pruning Weight. First consider optimizing Eq. 5 with respect to \mathbf{M}_ℓ and $\widehat{\mathbf{W}}_\ell$. For each linear layer ℓ in an FFN module, the optimal solution minimizes $\|\mathbf{z}_\ell - (\mathbf{M}_\ell \odot \widehat{\mathbf{W}}_\ell) \mathbf{a}_{\ell-1}\|_2^2$. In order to solve it, the first step is to write \mathbf{z}_ℓ as $\mathbf{W}_\ell \mathbf{a}_{\ell-1}$, where $\mathbf{W}_\ell = \mathbf{z}_\ell \mathbf{a}_{\ell-1}^\dagger$ (\dagger denotes the pseudo-inverse). We get $\|\mathbf{W}_\ell \mathbf{a}_{\ell-1} - (\mathbf{M}_\ell \odot \widehat{\mathbf{W}}_\ell) \mathbf{a}_{\ell-1}\|_2^2$ by plugging \mathbf{z}_ℓ back in the original loss. This aligns with the pruning objective of Eq. 2 and can be analytically solved by an existing pruning solver, for example, SparseGPT. The superscript of ‘‘pre’’ for $\mathbf{a}_{\ell-1}$ is omitted in this section for simpler notation.

Updating Activation. Minimization for \mathbf{a}_ℓ is a simple least-squares problem similar to weight pruning. In this case, however, the matrix $\mathbf{a}_{\ell-1}$ appears in two penalty terms in Eq. 5, so we must minimize $\alpha \|\mathbf{z}_{\ell+1}^{\text{pre}} - (\mathbf{M}_{\ell+1} \odot \widehat{\mathbf{W}}_{\ell+1}) \mathbf{a}_\ell\|_2^2 + \beta \|\mathbf{a}_\ell - \phi_\ell(\mathbf{z}_\ell)\|_2^2$ for \mathbf{a}_ℓ , holding all other variables fixed. By following an idea similar to Ridge regression, the new value of \mathbf{a}_ℓ is given by

$$(\alpha \mathbf{W}_{\ell+1}^\top \mathbf{W}_{\ell+1} + \beta \mathbf{I})^{-1} (\alpha \mathbf{W}_{\ell+1}^\top \mathbf{z}_{\ell+1}^{\text{pre}} + \beta \phi_\ell(\mathbf{z}_\ell)), \quad (6)$$

where \mathbf{W}_ℓ denotes the updated weight matrix after pruning, that is, $\mathbf{W}_\ell := \mathbf{M}_\ell \odot \widehat{\mathbf{W}}_\ell$.

Updating Output. The update for \mathbf{z}_ℓ requires minimizing the following loss:

$$\beta \|\mathbf{a}_\ell - \phi_\ell(\mathbf{z}_\ell)\|_2^2 + \alpha \|\mathbf{z}_\ell - (\mathbf{M}_\ell \odot \widehat{\mathbf{W}}_\ell) \mathbf{a}_{\ell-1}^{\text{pre}}\|_2^2. \quad (7)$$

This problem can be challenging because of the potentially nonlinear function $\phi_\ell(\cdot)$. Fortunately, since the nonlinearity $\phi_\ell(\cdot)$ between two consecutive FFN layers in the transformer is typically ReLU, which works entrywise on its argument, the entries in \mathbf{z}_ℓ are decoupled. As a result, solving Eq. 7 is particularly easy when ϕ_ℓ is piecewise linear (as in the case of ReLU). The equation can be solved in closed form following a simple if-then logic. Specifically, one needs only to compute two

solutions as

$$\begin{aligned} \mathbf{z}_\ell^{(1)} &= (\mathbf{M}_\ell \odot \widehat{\mathbf{W}}_\ell) \mathbf{a}_{\ell-1}^{pre}, \\ \mathbf{z}_\ell^{(2)} &= (\alpha + \beta)^{-1} \cdot (\beta \mathbf{a}_\ell + \alpha \mathbf{z}_\ell^{(1)}), \end{aligned} \quad (8)$$

where the first solution corresponds to those entries of \mathbf{z}_ℓ that are negative (reduced to zero by ReLU) and the second solution corresponds to those entries of \mathbf{z}_ℓ that are non-negative (i.e., $\phi_\ell(\mathbf{z}_\ell) = \mathbf{z}_\ell$). For more sophisticated choices of ϕ_ℓ , including smooth sigmoid curves, the problem can be solved quickly with a lookup table of precomputed solutions because each entry depends on only two inputs.

Remark 4.2 (Convergence to global optimum with AdaGP). *Consider the unconstrained problem given in Eq. 5. We observe that if the activation function ϕ is ReLU, (1) the objective function is convex with respect to each variable when all others are fixed and (2) closed-form solutions exist for each of the variable updates in the alternating optimization scheme. The proposed algorithm resembles a multiblock alternating direction method of multipliers that is shown to converge to the global optimum in many applications.*

4.4 Time Complexity Analysis

The proposed AdaGP is composed of three main steps, with the overall time complexity being the sum of the complexities of the individual steps. Consider one epoch of AdaGP. In the step of weights pruning, the time complexity is dominated by the computation of the pseudo-inverse of matrix \mathbf{a}_ℓ with dimensions $n \times h$ (where n is the number of samples and h is the hidden dimension of the transformer) and thus given by $O(nh^2)$, assuming $n < h$. The exact pruning step, when employing SparseGPT as the solver, has a complexity of $O(h^3)$. Combining both substeps, weight pruning has a total time complexity of $O(h^3)$. The second step, updating activation, is dominated by a matrix inversion as shown in Eq. 6. Given that the weight matrix \mathbf{W}_ℓ is of size $h \times h$, this inversion has a time complexity of $O(h^3)$. The third step, updating outputs, does not involve matrix inversion, and its complexity does not exceed that of the previous steps. Thus, the overall time complexity of the algorithm is bounded by $O(h^3)$. Consequently, our method exhibits a per-epoch time complexity that is on par with SparseGPT.

5 Experiments

Experiments Setup. We implement AdaGP in PyTorch (Paszke et al., 2019) and use the HuggingFace Transformers library (Wolf et al., 2019) for handling models and datasets. All pruning experiments are conducted on NVIDIA A100 GPUs. Similar to (Frantar and Alistarh, 2023; Sun et al., 2023), we sparsify each transformer decoder layer sequentially in order, which significantly reduces memory requirements, and apply global pruning only to FFN modules. For the calibration data, we follow Frantar and Alistarh (2023) and use 2048-token segments, randomly chosen from the first shard of the C4 (Raffel et al., 2020) dataset. This represents generic text data crawled from the Internet and ensures that our experiments remain zero-shot since no task-specific data is seen during pruning.

Models, Datasets, & Evaluation. Following (Frantar and Alistarh, 2023), we primarily work with the OPT model family (Zhang et al., 2022) to study scaling behavior at various model sizes, but our method can be easily applied to other LLMs such as Llama (Touvron et al., 2023). While our focus lies on the very largest variants, we also show some results on smaller models to provide a broader picture. In terms of metrics, we mainly focus on perplexity, which is known to be a challenging and stable metric that is well suited for evaluating the accuracy of compression methods (Yao et al., 2022; Dettmers and Zettlemoyer, 2023). We consider the test sets of raw WikiText-2 (Merity et al., 2016) and PTB (Marcus et al., 1994) as well as a subset of the C4 validation data, all popular benchmarks in the LLM compression literature (Yao et al., 2022; Park et al., 2022; Frantar and Alistarh, 2023; Sun et al., 2023). For additional interpretability, we also provide zero-shot accuracy results following the same setup of (Sun et al., 2023), which is based on the popular EleutherAI-eval harness (Gao et al., 2023).

Comparison Methods. We compare against the standard magnitude pruning baseline (Zhu and Gupta, 2017) applied locally. We also compare with two state-of-the-art local pruning methods, SparseGPT (Frantar and Alistarh, 2023) and Wanda (Sun et al., 2023).

5.1 Results and Analyses

Pruning vs. Model Sizes. We begin by exploring the pruning capabilities of AdaGP across various

OPT-1.3b (WikiText2: 14.62; PTB: 20.29; C4: 16.07)												
Sparsity	70%			80%			90%			2:4		
Dataset	WikiText-2	PTB	C4	WikiText-2	PTB	C4	WikiText-2	PTB	C4	WikiText-2	PTB	C4
Magnitude	6420.80	4828.13	3435.99	9998.71	1.1e4	5347.89	8209.13	1.0e4	4917.02	96.68	133.92	48.08
Wanda	21.56	34.77	25.78	142.20	146.76	142.24	5692.65	4751.69	4501.73	15.63	24.04	18.23
SparseGPT	18.04	28.19	21.45	69.67	93.36	60.83	2596.70	2361.86	1363.08	15.11	23.71	17.88
AdaGP	17.82	27.72	20.99	58.92	85.33	58.36	1350.31	1192.36	655.76	14.97	23.40	17.67
OPT-2.7b (WikiText-2: 12.47; PTB: 17.97; C4: 14.32)												
Sparsity	70%			80%			90%			2:4		
Dataset	WikiText-2	PTB	C4	WikiText-2	PTB	C4	WikiText-2	PTB	C4	WikiText-2	PTB	C4
Magnitude	1691.74	1237.08	1415.02	1.0e4	7916.69	6050.07	7.9e5	5.3e5	4.7e5	272.34	308.55	267.70
Wanda	88.61	140.09	90.06	6140.81	4746.96	5678.66	3.0e4	3.5e4	2.4e4	13.66	21.67	16.10
SparseGPT	13.79	21.18	16.18	24.32	37.82	25.92	2662.74	2285.01	1776.08	12.62	19.28	15.12
AdaGP	13.82	21.07	16.14	23.87	37.09	24.90	1200.12	759.11	527.70	12.63	19.31	15.12
OPT-6.7b (WikiText-2: 10.86; PTB: 15.77; C4: 12.71)												
Sparsity	70%			80%			90%			2:4		
Dataset	WikiText-2	PTB	C4	WikiText-2	PTB	C4	WikiText-2	PTB	C4	WikiText-2	PTB	C4
Magnitude	7054.21	5437.44	4850.25	7937.49	5971.86	6031.54	2.4e4	2.5e4	2.1e4	64.11	92.23	82.67
Wanda	54.95	129.73	116.67	1493.58	1196.93	996.00	2.1e4	2.0e4	1.8e4	11.86	18.54	14.77
SparseGPT	12.27	18.90	15.28	31.04	51.26	29.42	8871.24	5713.57	3797.20	11.30	16.90	13.51
AdaGP	12.16	18.39	14.93	23.96	39.32	26.97	2095.85	1842.48	953.44	11.07	16.73	13.42
OPT-13b (WikiText-2: 10.13; PTB: 14.52; C4: 12.06)												
Sparsity	70%			80%			85%			2:4		
Dataset	WikiText-2	PTB	C4	WikiText-2	PTB	C4	WikiText-2	PTB	C4	WikiText-2	PTB	C4
Magnitude	9037.12	7734.58	5909.47	1.1e4	9140.88	6340.22	1.3e4	1.3e4	9087.50	67.07	110.77	52.61
Wanda	30.94	39.26	33.31	4216.04	2894.77	2450.57	1.1e4	1.1e4	7244.96	10.33	15.35	12.54
SparseGPT	10.89	16.35	13.39	21.42	33.62	21.01	8408.03	6380.30	3416.23	10.20	15.14	12.48
AdaGP	10.96	16.57	13.38	19.07	28.77	19.29	2052.27	1536.51	538.61	10.21	15.15	12.48
OPT-30b (WikiText-2: 9.56; PTB: 14.04; C4: 11.45)												
Sparsity	70%			80%			90%			2:4		
Dataset	WikiText2	PTB	C4	WikiText-2	PTB	C4	WikiText-2	PTB	C4	WikiText-2	PTB	C4
Magnitude	8691.40	4769.89	4732.66	8941.81	5292.98	5092.26	3.8e7	3.0e7	1.4e7	517.71	374.54	991.95
Wanda	7766.61	5547.45	5741.74	8770.33	6020.70	7132.20	6354.15	4296.37	4654.27	10.94	16.64	13.50
SparseGPT	9.58	14.41	11.93	16.49	22.01	17.67	5747.87	5169.50	3555.24	9.59	14.05	11.60
AdaGP	9.56	14.40	11.94	15.61	19.64	16.61	3050.63	2712.39	1758.63	9.57	14.04	11.60
OPT-66b (WikiText-2: 9.34; PTB: 13.36; C4: 10.99)												
Sparsity	70%			80%			90%			2:4		
Dataset	WikiText-2	PTB	C4	WikiText-2	PTB	C4	WikiText-2	PTB	C4	WikiText-2	PTB	C4
Magnitude	OOM	OOM	OOM	OOM	OOM	OOM	OOM	OOM	OOM	OOM	OOM	OOM
Wanda	OOM	OOM	OOM	OOM	OOM	OOM	OOM	OOM	OOM	OOM	OOM	OOM
SparseGPT	9.45	13.64	11.37	28.27	57.41	26.26	7803.10	6594.88	4433.35	9.38	13.37	11.12
AdaGP	9.37	13.66	11.37	16.45	21.00	17.70	7504.17	5644.65	3683.91	9.36	13.36	11.12

Table 1: Perplexity of pruned OPT models in high sparsity regimes (> 60%); the lower the perplexity, the better.

model sizes in comparison with the baseline methods. For each model we consider unstructured sparsity ranging from 70% to 90% with a 10% increment, as well as a full 2:4 semi-structured sparsity. We conduct a sensitivity study on the calibration sample sizes (see Appendix A.4) and use calibration sample sizes between 32 and 64 for all experiments. Moreover, except for the OPT-125m model, we prune the first 50% of the transformer decoder layers in each model to achieve a balance between the computation resources and showcasing the performances. Detailed results can be found in Table 1

and Table 3 (see Appendix A.1). The perplexity results on the three datasets for the unpruned dense models are reported next to the names of the models. Note that we exclude the results for OPT-350m and adjust 90% unstructured sparsity for OPT-1.3b to 85% unstructured sparsity for numerical stability. We discuss the selection of hyperparameters of α and β (used in Eq. 5) in Appendix A.5.

The table shows that perplexity increases with increasing sparsity. Moreover, we observe a trend of decreasing perplexity for SparseGPT and AdaGP at the same sparsity with increasing model sizes.

OPT-6.7b									
Sparsity	Method	BoolQ	RTE	HellaSwag	WinoGrande	ARC-e	ARC-c	OBQA	Mean
Dense		66.12	56.03	50.49	65.27	65.72	30.63	27.60	51.69
70%	SparseGPT	61.74	54.87	48.46	63.85	64.31	29.27	25.40	49.70
	AdaGP	60.61	54.51	48.8	62.9	64.14	30.03	26.60	49.66
80%	SparseGPT	55.08	48.38	42.22	59.43	57.79	25.85	21.40	44.31
	AdaGP	58.69	51.26	43.78	59.67	58.38	26.88	22.00	45.81
90%	SparseGPT	38.53	53.07	26.00	48.07	26.81	21.67	14.40	32.65
	AdaGP	46.48	52.71	26.21	51.70	27.44	19.71	13.40	33.95
2:4	SparseGPT	62.11	54.87	49.58	64.4	65.32	30.63	27.60	50.64
	AdaGP	63.82	55.96	49.55	64.56	65.70	30.55	27.60	51.11

OPT-13b									
Sparsity	Method	BoolQ	RTE	HellaSwag	WinoGrande	ARC-e	ARC-c	OBQA	Mean
Dense		65.87	57.76	52.44	66.02	67.82	33.46	28.62	53.14
70%	SparseGPT	63.03	54.87	50.89	65.43	67.47	32.85	26.40	51.56
	AdaGP	63.85	55.23	50.73	65.67	66.46	31.83	27.20	51.57
80%	SparseGPT	59.72	52.35	46.82	61.48	62.50	31.23	21.80	47.99
	AdaGP	60.89	53.07	46.19	62.12	62.21	30.38	23.00	48.27
90%	SparseGPT	47.49	52.71	33.17	51.54	39.98	21.33	17.80	37.72
	AdaGP	53.43	52.71	38.19	52.96	46.68	25.26	17.40	40.95
2:4	SparseGPT	64.71	54.51	51.92	65.98	67.47	32.85	28.20	52.23
	AdaGP	65.63	55.23	51.93	65.27	67.8	33.45	28.40	52.53

OPT-30b									
Sparsity	Method	BoolQ	RTE	HellaSwag	WinoGrande	ARC-e	ARC-c	OBQA	Mean
Dense		70.46	61.82	54.27	69.02	70.47	35.49	30.20	55.96
70%	SparseGPT	68.78	58.48	53.83	67.64	69.15	34.30	29.60	54.54
	AdaGP	69.11	61.73	53.97	68.43	69.78	34.73	29.80	55.36
80%	SparseGPT	64.86	60.65	49.73	61.40	61.91	31.74	24.20	50.64
	AdaGP	65.41	59.57	50.65	61.96	62.71	32.25	26.50	51.29
90%	SparseGPT	37.83	53.79	25.96	49.88	26.47	20.22	12.60	32.39
	AdaGP	43.55	52.35	26.32	50.04	27.31	20.56	14.00	33.45
2:4	SparseGPT	69.54	58.12	54.08	67.25	69.95	34.81	29.80	54.79
	AdaGP	69.67	58.12	54.08	68.88	70.45	35.49	30.20	55.27

Table 2: Accuracy (%) of zero-shot tasks: the higher the accuracy, the better.

However, such a trend is not obvious for Magnitude and Wanda. We also observe that SparseGPT and AdaGP consistently outperform Magnitude and Wanda by a significant margin. For smaller sparsity, AdaGP achieves comparable perplexity to SparseGPT. As we increase the sparsity, AdaGP starts to demonstrate noticeable improvements over SparseGPT. In numerous instances, AdaGP achieves perplexity reductions of more than 50% compared with SparseGPT.

Computation Time vs. Model Sizes. Next, we study how the computation time for a single epoch of SparseGPT and AdaGP varies with different model sizes, as illustrated in Figure 3. We observe that the time taken for a single epoch increases with increasing model sizes. The rate at which the time taken increases is comparable for SparseGPT and AdaGP. Additionally, although SparseGPT executes only one epoch for each layer to prune, whereas AdaGP may execute multiple epochs depending on the parameter configuration, we find that in most cases few epochs (less than 10) of AdaGP suffice. This suggests that the proposed AdaGP remains computationally efficient.

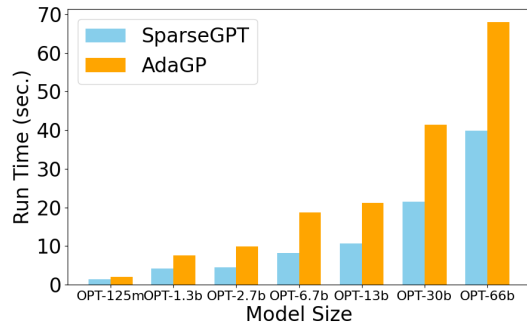


Figure 3: Time for one step of SparseGPT and AdaGP.

Zero-Shot Experiments. To conclude the evaluations and discussions, we show the results for several zero-shot tasks in Table 2 comparing SparseGPT and AdaGP and three model sizes. These evaluations are known to be relatively noisy (Dettmers et al., 2022) but more interpretable. We also report the results for zero-shot tasks from the unpruned dense models in the ‘‘Dense’’ row. We see that the accuracy of both methods decreases with increasing sparsity, which is expected, as more parameters are pruned. A similar trend of increasing accuracy with increasing model size is observed, too. Across all the tasks, OBQA and

ARC-c remain the most challenging ones as the accuracy for both methods remains around or below 30% while both methods perform well for BoolQ, RTE, WinoGrande, and ARC-e. In general, AdaGP is able to achieve higher accuracy in almost all tasks across the three models of different sizes.

6 Conclusion

Our work presents AdaGP, a cutting-edge framework poised to redefine the compression of LLMs through sparsity. By adeptly circumventing the scalability issues of global pruning and addressing the local suboptimality of existing methods, AdaGP stands as a significant advancement in the field. Our empirical results affirm its efficacy, particularly in high-sparsity environments, where it achieves a notable reduction in perplexity, thereby setting a new precedent for model compression. The versatility and minimal computational overhead of AdaGP complement its integration with current pruning technologies, underscoring its potential as a universal tool for enhancing the performance and accessibility of LLMs.

7 Limitations

While AdaGP marks a significant step forward in efficient pruning of large language models, we acknowledge the inherent trade-off associated with any model compression technique. First, while our method reduces the complexity of LLMs and enhances computational efficiency, there is an inevitable balance between sparsity and performance that requires careful calibration. Second, the effectiveness of AdaGP, similar to any pruning method, may vary across different models and tasks, and its generalizability to all scenarios remains an area for further exploration. Third, our approach assumes certain structural properties of the neural network, such as layerwise decomposability, which may not hold for all architectures. These limitations, while not undermining the contributions of AdaGP, suggest avenues for future research and refinement.

Acknowledgment

This research used resources of the Argonne Leadership Computing Facility at Argonne National Laboratory, which is supported by the Office of Science of the U.S. Department of Energy under contract DE-AC02-06CH11357. We gratefully acknowledge the computing resources provided on

Swing, a high-performance computing cluster operated by the Laboratory Computing Resource Center at Argonne National Laboratory.

Government license

The submitted manuscript has been created by UChicago Argonne, LLC, Operator of Argonne National Laboratory ("Argonne"). Argonne, a U.S. Department of Energy Office of Science laboratory, is operated under Contract No. DE-AC02-06CH11357. The U.S. Government retains for itself, and others acting on its behalf, a paid-up nonexclusive, irrevocable worldwide license in said article to reproduce, prepare derivative works, distribute copies to the public, and perform publicly and display publicly, by or on behalf of the Government. The Department of Energy will provide public access to these results of federally sponsored research in accordance with the DOE Public Access Plan (<http://energy.gov/downloads/doe-public-access-plan>)

References

- Guangji Bai, Zheng Chai, Chen Ling, Shiyu Wang, Jiaying Lu, Nan Zhang, Tingwei Shi, Ziyang Yu, Mengdan Zhu, Yifei Zhang, et al. 2024. Beyond efficiency: A systematic survey of resource-efficient large language models. *arXiv preprint arXiv:2401.00625*.
- Thomas Blumensath and Mike E Davies. 2008. Iterative thresholding for sparse approximations. *Journal of Fourier Analysis and Applications*, 14:629–654.
- Michael Bommarito II and Daniel Martin Katz. 2022. GPT takes the bar exam. *arXiv preprint arXiv:2212.14402*.
- Sébastien Bubeck, Varun Chandrasekaran, Ronen Eldan, Johannes Gehrke, Eric Horvitz, Ece Kamar, Peter Lee, Yin Tat Lee, Yuanzhi Li, Scott Lundberg, et al. 2023. Sparks of artificial general intelligence: Early experiments with gpt-4. *arXiv preprint arXiv:2303.12712*.
- Tim Dettmers, Mike Lewis, Younes Belkada, and Luke Zettlemoyer. 2022. LLM.int8(): 8-bit matrix multiplication for transformers at scale. *arXiv preprint arXiv:2208.07339*.
- Tim Dettmers and Luke Zettlemoyer. 2023. The case for 4-bit precision: k-bit inference scaling laws. In *International Conference on Machine Learning*, pages 7750–7774. PMLR.
- Elias Frantar and Dan Alistarh. 2023. Massive language models can be accurately pruned in one-shot. *arXiv preprint arXiv:2301.00774*.

- Leo Gao, Jonathan Tow, Baber Abbasi, Stella Biderman, Sid Black, Anthony DiPofi, Charles Foster, Laurence Golding, Jeffrey Hsu, Alain Le Noac'h, Haonan Li, Kyle McDonell, Niklas Muennighoff, Chris Ociepa, Jason Phang, Laria Reynolds, Hailey Schoelkopf, Aviya Skowron, Lintang Sutawika, Eric Tang, Anish Thite, Ben Wang, Kevin Wang, and Andy Zou. 2023. [A framework for few-shot language model evaluation](#).
- Song Han, Huizi Mao, and William J Dally. 2015. Deep compression: Compressing deep neural networks with pruning, trained quantization and Huffman coding. *arXiv preprint arXiv:1510.00149*.
- Torsten Hoefler, Dan Alistarh, Tal Ben-Nun, Nikoli Dryden, and Alexandra Peste. 2021. Sparsity in deep learning: Pruning and growth for efficient inference and training in neural networks. *The Journal of Machine Learning Research*, 22(1):10882–11005.
- Itay Hubara, Brian Chmiel, Moshe Island, Ron Banner, Joseph Naor, and Daniel Soudry. 2021. Accelerated sparse neural training: A provable and efficient method to find n: m transposable masks. *Advances in Neural Information Processing Systems*, 34:21099–21111.
- Jason Kingdon and Jason Kingdon. 1997. Hypothesising neural nets. *Intelligent Systems and Financial Forecasting*, pages 81–106.
- Eldar Kurtic, Elias Frantar, and Dan Alistarh. 2023. Zi-plm: Hardware-aware structured pruning of language models. *arXiv preprint arXiv:2302.04089*.
- Woosuk Kwon, Sehoon Kim, Michael W Mahoney, Joseph Hassoun, Kurt Keutzer, and Amir Gholami. 2022. A fast post-training pruning framework for transformers. *Advances in Neural Information Processing Systems*, 35:24101–24116.
- Yann LeCun, John Denker, and Sara Solla. 1989. Optimal brain damage. *Advances in neural information processing systems*, 2.
- Yixiao Li, Yifan Yu, Qingru Zhang, Chen Liang, Pengcheng He, Weizhu Chen, and Tuo Zhao. 2023. LoSparse: Structured compression of large language models based on low-rank and sparse approximation. *arXiv preprint arXiv:2306.11222*.
- Chen Ling, Xujiang Zhao, Jiaying Lu, Chengyuan Deng, Can Zheng, Junxiang Wang, Tanmoy Chowdhury, Yun Li, Hejie Cui, Tianjiao Zhao, et al. 2023. Domain specialization as the key to make large language models disruptive: A comprehensive survey. *arXiv preprint arXiv:2305.18703*, 2305.
- Zirui Liu, Qingquan Song, Qiang Charles Xiao, Sathya Keerthi Selvaraj, Rahul Mazumder, Aman Gupta, and Xia Hu. 2024. FFSplit: Split feed-forward network for optimizing accuracy-efficiency trade-off in language model inference. *arXiv preprint arXiv:2401.04044*.
- Xinyin Ma, Gongfan Fang, and Xinchao Wang. 2023. LLM-Pruner: On the structural pruning of large language models. *arXiv preprint arXiv:2305.11627*.
- Arun Mallya and Svetlana Lazebnik. 2018. Packnet: Adding multiple tasks to a single network by iterative pruning. In *Proceedings of the IEEE conference on Computer Vision and Pattern Recognition*, pages 7765–7773.
- Mitch Marcus, Grace Kim, Mary Ann Marcinkiewicz, Robert MacIntyre, Ann Bies, Mark Ferguson, Karen Katz, and Britta Schasberger. 1994. The Penn treebank: Annotating predicate argument structure. In *Human Language Technology: Proceedings of a Workshop held at Plainsboro, New Jersey, March 8-11, 1994*.
- Stephen Merity, Caiming Xiong, James Bradbury, and Richard Socher. 2016. Pointer sentinel mixture models. *arXiv preprint arXiv:1609.07843*.
- R OpenAI. 2023. Gpt-4 technical report. arxiv 2303.08774. *View in Article*, 2:13.
- Gunho Park, Baeseong Park, Se Jung Kwon, Byeongwook Kim, Youngjoo Lee, and Dongsoo Lee. 2022. nuQmm: Quantized matmul for efficient inference of large-scale generative language models. *arXiv preprint arXiv:2206.09557*.
- Adam Paszke, Sam Gross, Francisco Massa, Adam Lerer, James Bradbury, Gregory Chanan, Trevor Killeen, Zeming Lin, Natalia Gimelshein, Luca Antiga, et al. 2019. PyTorch: An imperative style, high-performance deep learning library. *Advances in Neural Information Processing Systems*, 32.
- Colin Raffel, Noam Shazeer, Adam Roberts, Katherine Lee, Sharan Narang, Michael Matena, Yanqi Zhou, Wei Li, and Peter J Liu. 2020. Exploring the limits of transfer learning with a unified text-to-text transformer. *The Journal of Machine Learning Research*, 21(1):5485–5551.
- Sidak Pal Singh and Dan Alistarh. 2020. Woodfisher: Efficient second-order approximation for neural network compression. *Advances in Neural Information Processing Systems*, 33:18098–18109.
- Shaden Smith, Mostofa Patwary, Brandon Norick, Patrick LeGresley, Samyam Rajbhandari, Jared Casper, Zhun Liu, Shrimai Prabhunoye, George Zerveas, Vijay Korthikanti, Elton Zhang, Rewon Child, Reza Yazdani Aminabadi, Julie Bernauer, Xia Song, Mohammad Shoeybi, Yuxiong He, Michael Houston, Saurabh Tiwary, and Bryan Catanzaro. 2022. [Using DeepSpeed and Megatron to Train Megatron-Turing NLG 530B, a large-scale generative language model](#).
- Mingjie Sun, Zhuang Liu, Anna Bair, and J Zico Kolter. 2023. A simple and effective pruning approach for large language models. *arXiv preprint arXiv:2306.11695*.

- Yi-Lin Sung, Jaehong Yoon, and Mohit Bansal. 2023. ECoFLaP: Efficient coarse-to-fine layer-wise pruning for vision-language models. *arXiv preprint arXiv:2310.02998*.
- Chaofan Tao, Lu Hou, Haoli Bai, Jiansheng Wei, Xin Jiang, Qun Liu, Ping Luo, and Ngai Wong. 2023. Structured pruning for efficient generative pre-trained language models. In *Findings of the Association for Computational Linguistics: ACL 2023*, pages 10880–10895.
- Hugo Touvron, Louis Martin, Kevin Stone, Peter Albert, Amjad Almahairi, Yasmine Babaei, Nikolay Bashlykov, Soumya Batra, Prajjwal Bhargava, Shruti Bhosale, et al. 2023. Llama 2: Open foundation and fine-tuned chat models. *arXiv preprint arXiv:2307.09288*.
- Shikhar Tuli and Niraj K Jha. 2023. AccelTran: A sparsity-aware accelerator for dynamic inference with transformers. *IEEE Transactions on Computer-Aided Design of Integrated Circuits and Systems*.
- Jason Wei, Yi Tay, Rishi Bommasani, Colin Raffel, Barret Zoph, Sebastian Borgeaud, Dani Yogatama, Maarten Bosma, Denny Zhou, Donald Metzler, et al. 2022. Emergent abilities of large language models. *arXiv preprint arXiv:2206.07682*.
- Thomas Wolf, Lysandre Debut, Victor Sanh, Julien Chaumond, Clement Delangue, Anthony Moi, Pierric Cistac, Tim Rault, Rémi Louf, Morgan Funtowicz, et al. 2019. Huggingface’s transformers: State-of-the-art natural language processing. *arXiv preprint arXiv:1910.03771*.
- Canwen Xu and Julian McAuley. 2023. A survey on model compression and acceleration for pretrained language models. In *Proceedings of the AAAI Conference on Artificial Intelligence*, volume 37, pages 10566–10575.
- Zhewei Yao, Reza Yazdani Aminabadi, Minjia Zhang, Xiaoxia Wu, Conglong Li, and Yuxiong He. 2022. Zeroquant: Efficient and affordable post-training quantization for large-scale transformers. *Advances in Neural Information Processing Systems*, 35:27168–27183.
- Susan Zhang, Stephen Roller, Naman Goyal, Mikel Artetxe, Moya Chen, Shuohui Chen, Christopher Dewan, Mona Diab, Xian Li, Xi Victoria Lin, et al. 2022. Opt: Open pre-trained transformer language models. *arXiv preprint arXiv:2205.01068*.
- Michael Zhu and Suyog Gupta. 2017. To prune, or not to prune: exploring the efficacy of pruning for model compression. *arXiv preprint arXiv:1710.01878*.

A Appendix

A.1 OPT-125m

Detailed results for OPT-125m are in Table 3. For a thorough investigation, we additionally consider unstructured sparsity of 50% and 60% as well as pruning the full model (instead of the first 50% of the transformer decoder layers). Similar to other models, we report the perplexity results for the unpruned dense model next to the name of the model in the table. In particular, we see that SparseGPT and AdaGP outperform Magnitude and Wanda with a significant margin across different levels of sparsity. AdaGP achieves similar perplexity with SparseGPT at smaller sparsity but demonstrates much better perplexity for larger sparsity. Similar perplexity trends are observed across the three datasets, although PTB, having the highest perplexity for each sparsity and method, seems to be the most challenging dataset among the three.

OPT-125m (WikiText2: 27.66; PTB: 38.99; C4: 26.56)									
Sparsity	Method	WikiText-2	PTB	C4	Sparsity	Method	WikiText2	PTB	C4
50%	Magnitude	193.39	276.33	141.03	80%	Magnitude	4890.96	4121.49	3213.85
	Wanda	39.58	57.44	35.12		Wanda	1912.45	2512.93	1066.86
	SparseGPT	37.49	55.91	33.63		SparseGPT	2072.12	1952.85	1050.83
	AdaGP	37.09	55.82	33.40		AdaGP	1358.10	1418.09	654.54
60%	Magnitude	920.29	1146.49	598.45	90%	Magnitude	6613.18	5380.80	4475.29
	Wanda	76.30	106.92	61.33		Wanda	4940.89	4337.27	3126.02
	SparseGPT	62.22	87.70	49.85		SparseGPT	6131.57	6963.27	2443.33
	AdaGP	59.28	84.36	47.78		AdaGP	5291.64	5067.41	2003.09
70%	Magnitude	3806.96	3429.35	2263.37	2:4	Magnitude	342.51	798.99	223.19
	Wanda	351.83	412.52	248.94		Wanda	83.81	113.01	65.78
	SparseGPT	239.26	265.83	156.33		SparseGPT	61.44	92.30	51.42
	AdaGP	208.46	255.75	137.72		AdaGP	56.55	81.46	46.14

Table 3: Perplexity on pruned OPT-125m: the lower the perplexity, the better

A.2 Pseudo-code of AdaGP

Algorithm 1 Adaptive Global Pruning for the FFN Module of an LLM.

Input: Pretrained weight matrices \mathbf{W}_ℓ and $\mathbf{W}_{\ell+1}$, inputs $\mathbf{a}_{\ell-1}^{pre}$ and \mathbf{a}_ℓ^{pre} , and outputs \mathbf{z}_ℓ^{pre} and $\mathbf{z}_{\ell+1}^{pre}$ for FFN’s upscaling and downscaling layers ℓ and $\ell + 1$; target sparsity ρ ; constraint weight hyperparameters α, β .

```

1 AdaGP () :
2   Initialize  $\mathbf{z}_\ell = \mathbf{z}_\ell^{pre}, \mathbf{a}_\ell = \mathbf{a}_\ell^{pre}$  ▷ Initialize slack variables
   Precompute and cache  $\mathbf{a}_{\ell-1}^\dagger = \text{pseudo-inverse}(\mathbf{a}_{\ell-1}^{pre})$ 
   for step  $i = 1, \dots, K$  do
3      $\mathbf{W}_\ell = \mathbf{z}_\ell \mathbf{a}_{\ell-1}^\dagger, \mathbf{W}_{\ell+1} = \mathbf{z}_{\ell+1}^{pre} \mathbf{a}_\ell^\dagger$ 
      $\mathbf{M}_\ell, \widehat{\mathbf{W}}_\ell = \arg \min \|\mathbf{W}_\ell \mathbf{a}_{\ell-1}^{pre} - (\mathbf{M}_\ell \odot \widehat{\mathbf{W}}_\ell) \mathbf{a}_{\ell-1}^{pre}\|_2^2$  ▷ Prune layer  $\ell$  by SparseGPT solver
      $\mathbf{M}_{\ell+1}, \widehat{\mathbf{W}}_{\ell+1} = \arg \min \|\mathbf{W}_{\ell+1} \mathbf{a}_\ell - (\mathbf{M}_{\ell+1} \odot \widehat{\mathbf{W}}_{\ell+1}) \mathbf{a}_\ell\|_2^2$  ▷ Prune layer  $\ell + 1$  by SparseGPT solver
      $\mathbf{W}_{\ell+1} = \mathbf{M}_{\ell+1} \odot \widehat{\mathbf{W}}_{\ell+1}, \mathbf{W}_\ell = \mathbf{M}_\ell \odot \widehat{\mathbf{W}}_\ell$ 
      $\mathbf{a}_\ell = (\alpha \mathbf{W}_{\ell+1}^\top \mathbf{W}_{\ell+1} + \beta \mathbf{I})^{-1} (\alpha \mathbf{W}_{\ell+1}^\top \mathbf{z}_{\ell+1}^{pre} + \beta \phi_\ell(\mathbf{z}_\ell))$  ▷ Update activations
      $\mathbf{z}_\ell^{(1)} = \mathbf{W}_\ell \mathbf{a}_{\ell-1}^{pre}, \mathbf{z}_\ell^{(2)} = (\alpha + \beta)^{-1} \cdot (\beta \mathbf{a}_\ell + \alpha \mathbf{z}_\ell^{(1)})$ 
     for  $j = 1, \dots, n$  in parallel do
4       if  $(\mathbf{z}_\ell)_j < 0$  then
5          $(\mathbf{z}_\ell)_j = (\mathbf{z}_\ell^{(1)})_j$  ▷ Update outputs
6       else
7          $(\mathbf{z}_\ell)_j = (\mathbf{z}_\ell^{(2)})_j$  ▷ Update outputs
8   return  $\mathbf{W}_\ell, \mathbf{W}_{\ell+1}$ 

```

The adaptive global pruning (AdaGP) algorithm presented in Algorithm 1 focuses on the optimization of the feed-forward network (FFN) module within a large language model (LLM). The key inputs to

the algorithm include the pretrained weight matrices, inputs and outputs for both the upscaling and downscaling linear layers of the FFN, along with a set of hyperparameters and a target sparsity. The goal of AdaGP is to achieve a targeted level of sparsity in the linear layers without significantly compromising the model’s performance.

Initiating with the pretrained weights, AdaGP employs a series of pruning and activation update steps across K epochs. In each epoch, it solves optimization problems to prune the weights in both upscaling and downscaling layers, followed by updating the activation variables. The utilization of SparseGPT solver for pruning and the strategic update of activations ensure that the pruned network behaves as similarly as possible to that of the original network. The final output of the algorithm is a pair of pruned weight matrices for the consecutive layers, which are expected to deliver comparable, if not improved, performance with a reduced number of nonzero parameters.

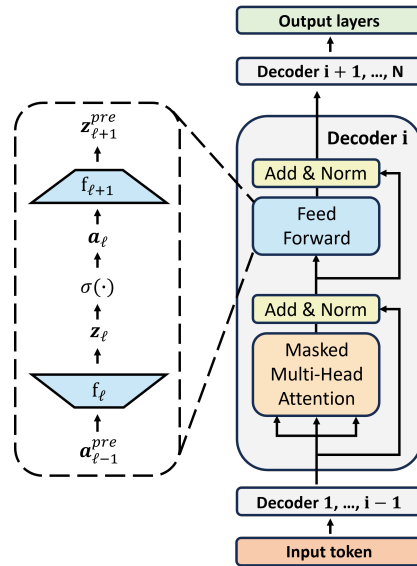


Figure 4: Visualization of the AdaGP algorithm applied to the FFN module in a transformer decoder. This diagram illustrates the flow of data through the layers of the decoder, where AdaGP performs global pruning to enhance sparsity and computational efficiency without compromising the model’s performances. Each decoder layer is shown with its core components: Masked Multi-Head Attention and Feed Forward network, with AdaGP focusing on the latter for pruning. For other linear layers outside of the FFN modules, AdaGP follows the same local pruning as SparseGPT does to prune them.

A.3 Visualization of AdaGP for FFN Global Pruning

Figure 4 presents a schematic representation of the AdaGP algorithm applied to the FFN module within a transformer model’s decoder layer. This visualization highlights the process of global pruning applied to the FFN module, aimed at reducing the model’s complexity while preserving its ability to capture essential patterns in the data.

The AdaGP method operates within the decoder block, selectively pruning the weights of the FFN module. Each decoder block comprises a series of operations. It starts with masked multihead attention and follows by additive normalization. Subsequently, it passes through the feed-forward network in which the pruning happens with AdaGP. The figure illustrates the flow of information from an input token through successive layers of the decoder. AdaGP not only enhances computational efficiency but also has the potential to improve model generalization by eliminating redundant parameters.

A.4 Calibration Samples

Figure 5 presents how perplexity changes with the calibration sample sizes on the datasets PTB and C4, respectively. On the one hand, in both plots, as the number of calibration samples increases, the perplexity decreases for both SparseGPT and AdaGP. This suggests that having more calibration samples

can be beneficial in the pruning process. Perplexity decreases more rapidly from 8 samples to 32 samples. Beyond 32 samples, the rate at which perplexity decreases starts to slow down. For PTB dataset, the perplexity even increases from 64 samples to 128 samples. On the other hand, increasing the number of calibration samples requires more computational resources, for example, memory and computation time, in the execution. A calibration sample size between 32 and 64 can therefore strike a balance between good performance and computational efficiency. We point out that the figures show that AdaGP starts to achieve better perplexity than SparseGPT does from 32 samples and remains better for 64 and 128 samples.

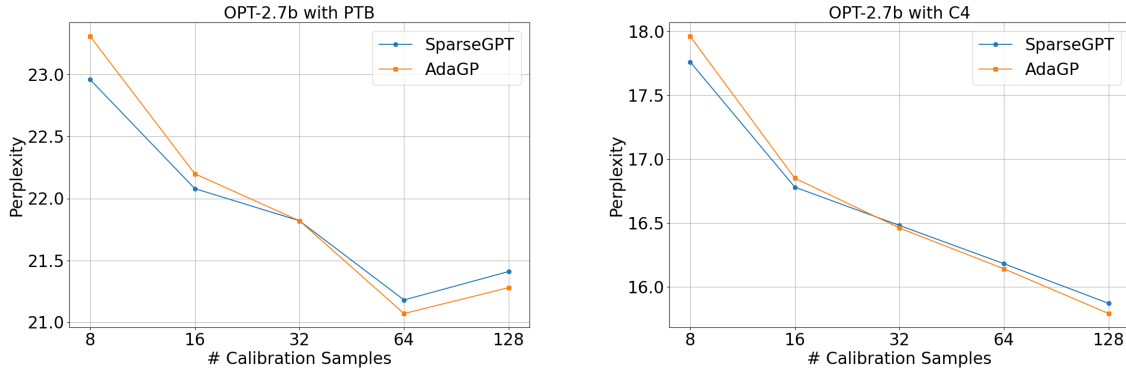


Figure 5: Sensitivity of OPT-2.7b on the calibration sample sizes for datasets PTB and C4.

A.5 Hyperparameter α and β Selection

Hyperparameters α and β are used in Eq. 5. We select α and β from the set $\{0.1, 1.0, 5.0\}$ and perform a study on model OPT-2.7b to understand the impact of the hyperparameters. We determine that $\alpha = \beta = 0.1$ give the best and numerically stable performances.